e-ISSN: 2582-5208
International Research Journal of Modernization in Engineering Technology and Science
(Peer-Reviewed, Open Access, Fully Refereed International Journal)
Volume:05/Issue:10/October-2023 Impact Factor- 7.868 www.irjmets.com

MRI-BASED BRAIN TUMOR SEGMENTATION BASED ON CROSS-MODAL DISTILLATION

Priya Dharshini MV*1, Nantha Priya NR*2

*1,2Department Of ECE, Vins Christian College Of Engineering, India.

DOI : https://www.doi.org/10.56726/IRJMETS45028

ABSTRACT

Clinical picture examination's vital work of sectioning cerebrum growths is significant since it assists with recognizing and track diseases of the mind. Notwithstanding, because of the muddled and confounding nature of the growth locale, dependably distinguishing and sectioning cerebrum cancers from attractive reverberation imaging (X-ray) keeps on being troublesome. In this paper, we recommend a clever strategy for portioning mind cancers named the Double Unraveling Organization (DDN), which utilizes the strength of unraveled portrayals to further develop division accuracy. The Element Unraveling Module (FDM) and the Division Module (SM) are the two interrelated modules that make up the DDN. The FDM is made to isolate the qualities of the information picture into different unraveled portrayals, every one of which addresses an alternate part of it, like the boundaries, surfaces, and foundation of the growth. The SM then, at that point, performs division utilizing a U-Net engineering on these de-ensnared portrayals. Unraveling permits the DDN to focus on significant highlights and effectively recognize the cancer district from solid mind tissue, creating division discoveries that are more exact and dependable. On a sizable dataset of cerebrum X-ray filters with distinguished growth regions, we evaluated our proposed approach and stood out it from other state of the art division models. As per the exploratory discoveries, the Double Unraveling Organization performs better compared to different techniques as far as division accuracy and speculation power.

Keywords: Magnetic Resonance Imaging, Brain Tumor, Feature Distillation, Quantitative Analysis, Image Processing.

I. INTRODUCTION

The conclusion of essential cerebrum growths and the help of quantitative examination, (for example, radiomics) for follow-up and treatment arranging require the division of the mind cancer. A computerized division arrangement is alluring on the grounds that manual division requires some investment and is vulnerable to between spectator fluctuation. For X-ray based cerebrum cancer division, profound learning models utilizing convolutional brain organizations (CNNs) have delivered superb outcomes. In any case, most of state of the art CNN models were made with the assumption that dependable arrangements of X-ray groupings would be available for both preparation and deduction. Utilizing whole arrangements of T1-weighted (T1w), contrast improved T1-weighted (T1ce), T2-weighted (T2w), and Liquid Constriction Reversal Recuperation (Pizazz) X-ray groupings, for example, is the Multimodal Cerebrum Growth Division (Whelps) benchmark. Therefore, these total sets are used by all highest level CNN-based methods for both preparation and derivation.

In any case, the quantity of X-ray arrangements that can be utilized for every patient in clinical practice changes more. A portion of the reasons for the shortfall of X-ray successions incorporate lacking filtering time, conflicting examining settings (for instance, because of convention breaks), or picture defilements (for example, because of patient movement). Furthermore, because of an absence of normalization, the image qualities and nature of X-ray outputs could change fundamentally among scanners and imaging offices. Thus, precise demonstrative surmising in a certifiable clinical circumstance is significantly more troublesome. Clinical X-ray information are possibly incongruous with the reference preparing information. The accessibility of T1ce succession information, which thusly requires the infusion of difference specialists (like Gadolinium), is vital for the exact division of some growth sub-districts, for example, the cancer center. Contrast synthetic compounds can expand the absolute examining time and put patients at higher gamble while additionally making the growth center considerably more apparent and making it simpler to outline the practical cancer.

The adequacy of a few created CNN models for X-ray based cerebrum growth division can be undermined by the issue of missing X-ray successions, all the more eminently contrast-improved X-ray groupings, which

e-ISSN: 2582-5208
International Research Journal of Modernization in Engineering Technology and Science
(Peer-Reviewed, Open Access, Fully Refereed International Journal)
Volume:05/Issue:10/October-2023 Impact Factor- 7.868 www.irjmets.com

subsequently restricts their useful application. To get around this issue, we made a cross-modular refining technique that utilizations full arrangements of X-ray groupings for preparing to improve division execution on a more modest arrangement of X-ray successions for induction. This is predictable with the Whelps drive's creating research objective, which plans to expand the adaptability of CNN models for clinical picture handling so these techniques can all the more likely handle missing information.

II. LITERATURE REVIEW

Roy, et al. have proposed Human Mind Attractive Reverberation (MR), In this examination, they propose a scanty word reference learning system and map book priors-based fix based tissue order strategy from MR pictures. A map book MR picture, earlier data maps showing the areas of different tissues that are expected to be available, and a hard division act as the technique's preparation information. X-ray can recognize fat, water, muscle, and other delicate tissue and has unrivaled differentiation for delicate tissue than CT. The X-ray process takes additional time than the CT cycle.

Dubey, et al. present Intuitionistic Fluffy sets and unpleasant sets are broadly utilized for clinical picture division, For dividing the attractive reverberation (MR) mind pictures For fragmenting the attractive reverberation (MR) mind pictures, a harsh set based intuitionistic fluffy c-implies (RIFCM) grouping method is proposed in this article. The natural fluffy set (Uncertainties) is an adaptable model that can be utilized to explain the vulnerability and uncertainty innate in navigation. The issue of information unevenness has for some time been an issue for mind cancer division.

Zhang, et al. The capacity of primary attractive reverberation imaging (X-ray) to analyze Alzheimer's sickness (Promotion) has been illustrated. A longitudinal report is more delicate in identifying early neurotic modifications of Promotion than a customary X-ray based Promotion finding, making it more helpful for exact conclusion. customary X-ray based Promotion determination ordinarily utilizes pictures taken at a solitary time point. It can describe the life systems of the human cerebrum without intercession on account of underlying X-ray. Despite the fact that X-ray isn't awkward, the people who are claustrophobic may find it challenging to sit still in an encased scanner.

Dong, et al. have proposed neighborhood inclination field assessment (LBFE), They propose a functioning form model in view of nearby predisposition field assessment (LBFE) to resolve this issue, working on the model's capacity to portion complex pictures. One frequently utilized procedure for sectioning pictures is the dynamic shape model. Most dynamic form models currently being used give inferior division results when utilized on confounded pictures, for example, those with grayscale consistency. To fundamentally build strength and tight the division range, a new variational level set capability is created. Harmful cancers and harmless illnesses are at times hard for X-ray to separate.

Pereira, et al. Convolutional Brain Organizations' idea, with regards to picture classification with convolutional brain organizations, press and excitation blocks were created to become familiar with the between channel communications and recalibrate the channels to smother the less significant ones. With regards to picture classification with convolutional brain organizations, crush and excitation blocks were created to gain proficiency with the between channel connections and change the channels to stifle the less significant ones. CNN offers a division free methodology that gets rid of the need for physically made include extractor strategies. The way that CNNs need a great deal of named information to prepare well, which can be costly and tedious to assemble and clarify, is one of their key downsides.

As indicated by the subregion order, the fountain is planned to separate the multi-class division issue into a progression of three double division issues. Consequently, Wang, et al. have proposed Multi-Modular Attractive Reverberation (MR), To isolate multi-modular attractive reverberation imaging (MR) pictures of cerebrum cancers into foundation and three progressive locales — the general growth, the growth center, and the upgrading cancer center — an outpouring of completely convolutional brain networks is introduced. Any part of the body can be imaged involving a X-ray scanner in any imaging heading. Attractive materials will be pulled by a X-ray scanner, which could bring about the clinical contraption moving unexpectedly.

Isensee, et al. propose a Glioblastoma division, Convolutional brain networks are utilized in cutting edge draws near, albeit regularly a couple of layers and thin open fields are utilized, restricting the amount and type of

e-ISSN: 2582-5208
International Research Journal of Modernization in Engineering Technology and Science
(Peer-Reviewed, Open Access, Fully Refereed International Journal)
Volume:05/Issue:10/October-2023 Impact Factor- 7.868 www.irjmets.com

context oriented information that can be divided. Rapid cancer discovery is conceivable with further developed precision. It offers robotization in the space of picture handling, examination, and further develops cerebrum structure acknowledgment in clinical science. an absence of coordination or unfortunate equilibrium. Changes in conduct or character.

III. EXISTING SYSTEM

In this proposed system a dual disentanglement framework (D2-Net) consisting of the MD-Stage and TD-Stage to handle the issue of missing modalities in brain tumor segmentation. The MD-Stage helps the model explicitly exploit the correlations among modality-specific information by decomposing them from MRI images, and the TD-Stage produces decoupled tumor-specific knowledge unrelated to MRI modalities, which can address the missing modality issue. In summary, this work includes three major contributions:

In contrast to prior arts that implicitly learn modality relations among multi-modal MRI images in the feature space, propose a novel SFMC learning scheme in the MD- Stage to explicitly decouple the modality-specific information from MRI images and exploit the correlations among modality representations in a content-independent modality space.

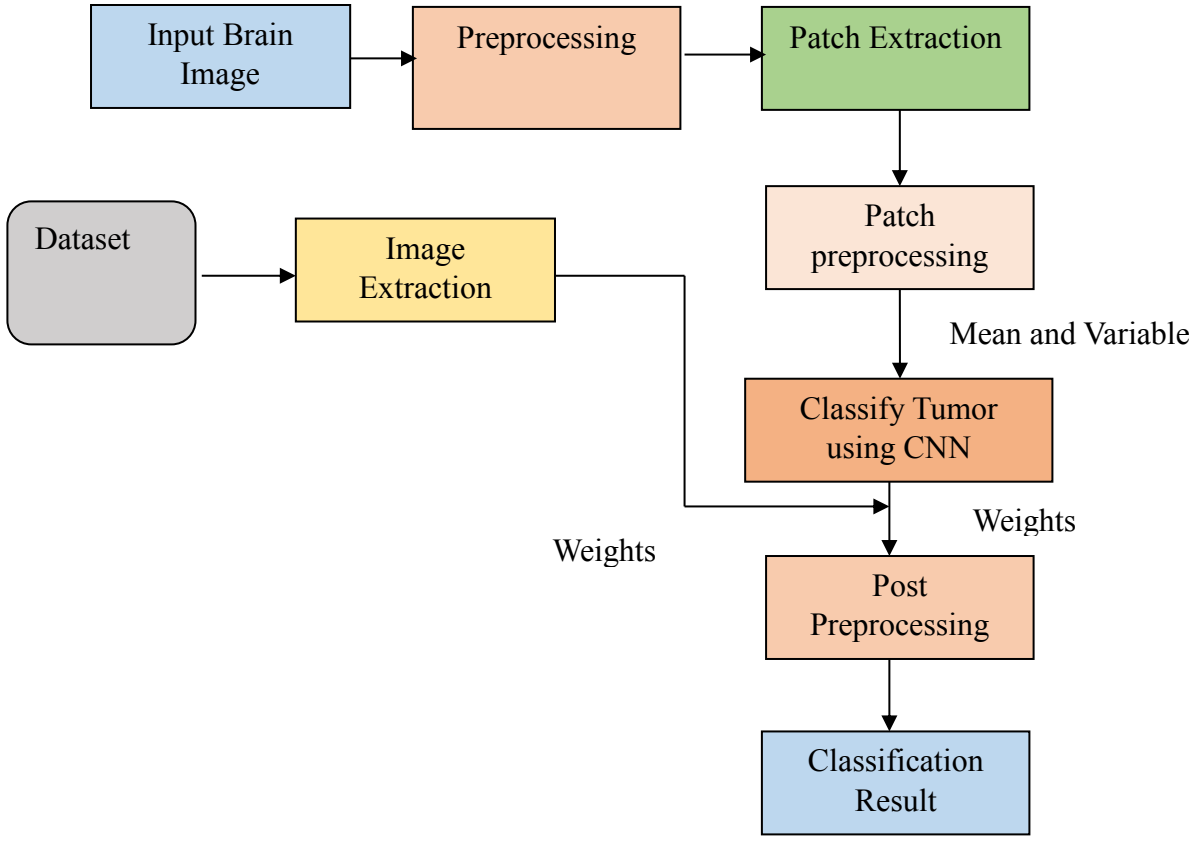

Figure 1: Block Diagram of Existing System

Represent the first effort to decouple features into multiple individual tumor-specific features in the TD-Stage. To provide tumor-specific supervision and enable accurate tumor-region disentanglement, an ADT-KD mechanism is designed to align the features of a disentangled binary teacher with a holistic student networks. Conduct extensive experiments on a challenging brain tumor segmentation dataset BraTS-2018 and demonstrate a clear advantage of the proposed framework over stateof-the-art methods in missing modalities situations. This work, proposes a dual disentanglement network (D2-Net) for brain tumor segmentation with missing modalities, as illustrated.

It consists of a modality disentanglement stage (MD-Stage) for modality-specific information decoupling and a tumor-region disentanglement stage (TD-Stage) for tumor-specific knowledge separation. In the MD-Stage, D^2-Net takes the MRI image x with multi-modalities as inputs to obtain fused tumor feature z via the tumor encoder E_T. Meanwhile, each modal image is separately input the corresponding modality encoders E_M with a

e-ISSN: 2582-5208
International Research Journal of Modernization in Engineering Technology and Science
(Peer-Reviewed, Open Access, Fully Refereed International Journal)
Volume:05/Issue:10/October-2023 Impact Factor- 7.868 www.irjmets.com

global average pooling (GAP) layer to produce the modality-specific codes c under the constraint of subtly designed spatial-frequency jointly modality contrastive (SFMC) learning scheme. The disentangled modality-specific codes c are then transferred to desired tumor-specific codes ĉ via a tumor modality projection network E_{TM} to discover the correlations among modalities and tumor-region features in the latent space. In the TD-Stage, the modality-content reconstruction network E_R transfers the tumor feature z and tumor-specific codes ĉ into tumor-specific features F. The tumor-region features F are decoupled via a disentangled binary decoder D^T and then boost the holistic features through a novel affinity-guided dense tumor-region knowledge distillation (ADT-KD) mechanism with a holistic multi-class tumor-region decoder DS and the disentangled binary decoder D^T. Finally, the brain tumor segmentation is obtained by holistic tumor-region student D^S. The overall network is optimized by joint loss functions including the proposed SFMC loss (L_{SFMC}), ADT-KD loss (L_{ADT-KD}), one reconstruction loss (L_{rec}), one consistency loss (L_{consis}), one binary cross-entropy loss (L_{aux}) and one standard segmentation loss (L_{seg}).

IV. PROPOSED SYSTEM

The educator network is addressed by the orange box in the proposed information refining design, and the understudy network is addressed by the blue box. The picture they utilized as information was something very similar. The cross-modular element refining (FD) module and the information refining (KD) module are situated in the green box that isolates the two organizations. The understudy model is prepared to repeat the information procured by the instructor model inside the Educator Understudy structure with the goal that the expectations made by the two models agree. This was at first finished via preparing the understudy model by limiting the cross-entropy misfortune capability while utilizing the back class probabilities of the educator model as targets. Nonetheless, the mellowed results don't precisely match the educator's learnt middle of the road include portrayals. Thus, middle oversight was added to the information refining idea to make a more broad system and synchronize the moderate enactment maps between the teacher and understudy model.

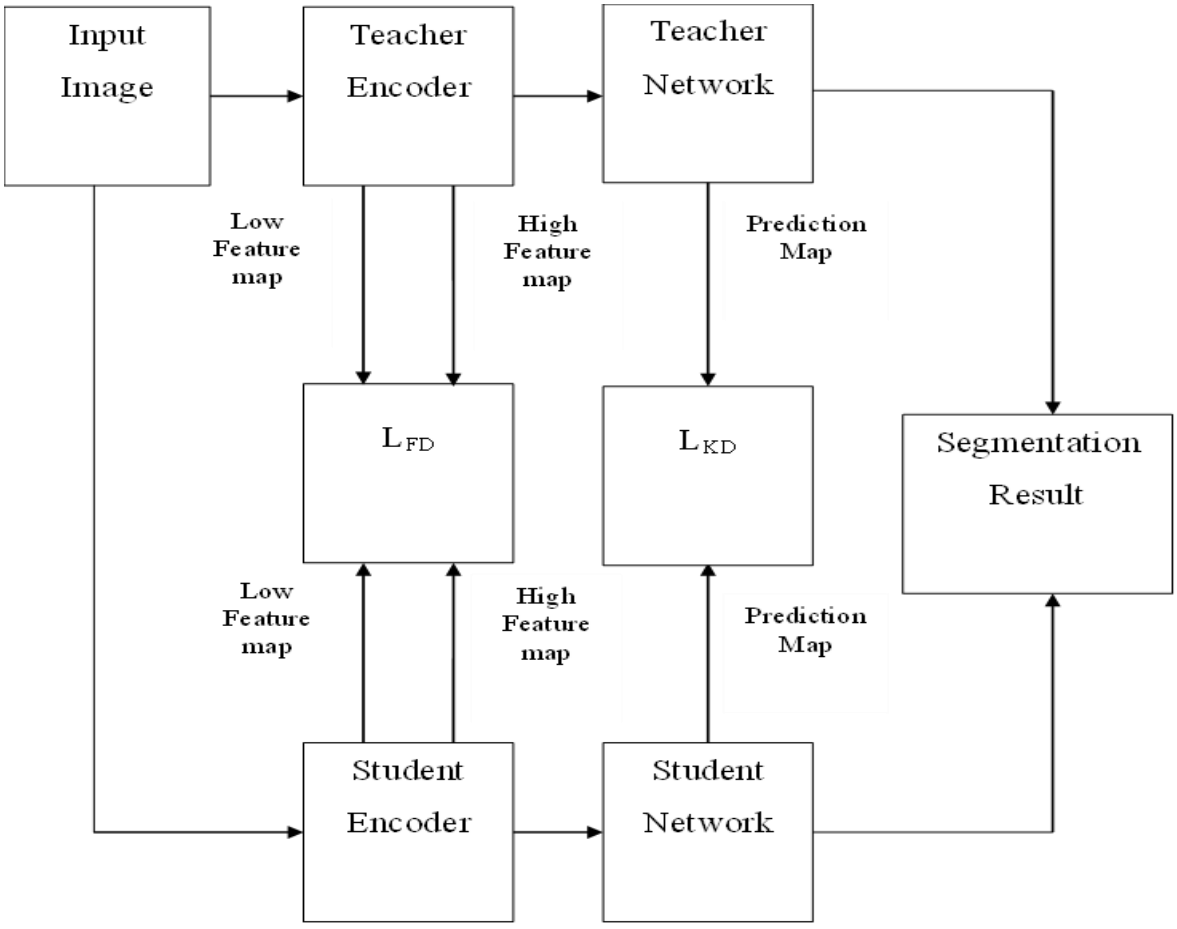

Figure 2: Proposed System Block Diagram

e-ISSN: 2582-5208
International Research Journal of Modernization in Engineering Technology and Science
(Peer-Reviewed, Open Access, Fully Refereed International Journal)
Volume:05/Issue:10/October-2023 Impact Factor- 7.868 www.irjmets.com

To prepare the understudy model, two systems were thought about for this review: (I) cross-modular information refining (KD), where just the educator's mellowed results were utilized; and (ii) cross-modular component refining (F D), where extra oversight was utilized to upgrade the middle of the road highlight portrayals of the understudy model.

4.1. Input Picture

The division of the whole growth and the cancer center created by the different CNN models utilizing the Whelps 2018 test dataset. T1w, T2w, and F Refuge sequencing information are utilized as contribution to a U-Net model for whole cancer division.

4.2. Teacher-Understudy Model

Through considering the expected division names by the educator and the connected ground truth marks, the educator model was prepared without any preparation in the main stage. The "Educator Understudy" model was mutually enhanced in the subsequent stage, with the educator model being set in a frozen state and its loads being used to introduce the understudy model's loads. For the job of whole cancer division and the errand of growth center division, the educator model was prepared utilizing T2 or potentially F Den arrangement information. The educator model's loads were utilized to introduce the understudy model, which was then prepared utilizing T1 succession information.

4.3. Cross-Modular Information Refining

They conceived a two-stage preparing strategy for the KD procedure, where the main stage included freely preparing the educator model and the subsequent step included mutually preparing the "Instructor Understudy" model. Utilizing consider the anticipated division names by the educator, yT,i, and the matching ground truth marks, yi, and limiting the delicate Dice misfortune, the instructor model was prepared without any preparation in the main stage.

$$L_{SD} = 1 - \frac{2\sum y_i\, y_{T,i}}{\sum y_i + \sum y_{T,i}}$$

It has been exhibited that further developing the delicate Dice scores during surmising by restricting the delicate Dice misfortune during preparing. The "Educator Understudy" model was mutually enhanced in the subsequent stage, with the educator model being set in a frozen state and its loads being used to introduce the understudy model's loads. Since the refining from the educator model to the understudy model was unidirectional, the understudy model's streamlining made little difference to the instructor model. This prompted the KD approach's goal capability being as per the following.

$$L_{KD}(\alpha, T) = (1-\alpha)L_{SD-S} + \alpha T^2 H(\sigma\left(\frac{Z_T}{T}\right), \sigma(\frac{Z_S}{T})$$

Z_Tand Z_S represented the logits delivered by the educator and understudy models, individually; H represented the cross-entropy capability; T represented the temperature boundary to mellow the names; S represented the sigmoid or softmax capability; and S represented a boundary to adjust the heaviness of the instructor's delicate marks with that of the hard marks from the beginning. The understudy model's projected division marks, y_(S,i), and the relating ground truth names, y_i, were matched by the delicate Dice misfortune L_(SD-S).

$$L_{SD-S} = 1 - \frac{2\sum y_i\, y_{S,i}}{\sum y_i + \sum y_{S,i}}$$

As a result, the KD approach's objective function included cross-entropy with soft-dice loss, which has shown to be effective for a variety of segmentation problems.

4.4. Cross-Modal Feature Distillation

The concepts of "hint-learning," in which "hint" refers to the feature representation in a middle layer of the instructor model, introduced the concept of "feature distillation." The following can be used to create the general objective function for feature distillation.

$$L_{distill} = D(f_T\left(F_T(l), f_S\left(F_S(l)\right)\right)$$

e-ISSN: 2582-5208
International Research Journal of Modernization in Engineering Technology and Science
(Peer-Reviewed, Open Access, Fully Refereed International Journal)
Volume:05/Issue:10/October-2023 Impact Factor- 7.868 www.irjmets.com

with f_T and f_S as the change capabilities to adjust the comparing highlight portrayals, and F_T and F_S as the relating highlight portrayals of the educator and understudy models in the go-between or somewhere in the vicinity called directing layer l. A distance metric D is utilized to look at how comparative the educator and understudy models' particular element portrayals are to each other.

The refining position, the decision of the directing layer, the change capabilities, and the distance metric are the significant parts of an element refining methodology. Different element refining executions can be thought about relying upon these choices. Convolution, normalizing, and ReLU make up a standard convolution block, and refining is commonly utilized after ReLU toward the finish of the block. This purported post-actuation pose just exchanges positive qualities for information refining since ReLU sift through bad qualities.

The contrary procedure, known as the "Pre-ReLU position," jam both the positive and negative qualities by playing out the refining before ReLU. To guarantee that critical data that might be available in both positive and negative qualities gets conveyed, a reasonable change capability and distance metric should be determined relying upon which refining position is picked. FitNet arrived at the midpoint of the neuron reaction all through the channel aspect while consideration move (AT) moved the full neuron reaction in the mediator layer to forestall data misfortune. Then again, refining of enactment limits (Stomach muscle) lost the element values since it utilized a binarized type of the component portrayal.

To keep up with both positive qualities and an edge with negative qualities, Redesign of Element Refining (OFD) utilized an edge ReLU as the essential change capability. Albeit the l2 standard keeps on being the most generally used distance metric for highlight refining, numerous adjustments of the l2 standard were additionally thought about in light of the refining area and the educator and understudy change capability. The enactment levels were non-straightly standardized involving the sigmoid capability as a change capability for both the teacher and understudy models. Like other standardization strategies, this accelerated preparation while balancing out the educational experience. The closeness between the component portrayal of the teacher and understudy models was additionally estimated utilizing the l2 standard.

In spite of the possibility of constant refining, the proposed F D method was carried out as an underlying refining that main applies refining in the beginning phase of preparing. Except for the subsequent stage, which was partitioned into two phases as per the recently distributed two-stage preparing, the preparation program for the F D was thusly tantamount to that for the KD. To have the understudy model mirror the transitional portrayal of the educator model at the halfway layer l, the "Instructor Understudy" model was mutually prepared up to the directing layer l during the primary stage. The objective capability for the principal stage was more exact when the squared l2 standard was utilized as the distance metric and the sigmoid capability as the change capability.

$$L_{l2}(l) = \frac{1}{2}\left\|\sigma\left(A_T(l)\right) - \sigma\left(A_S(l)\right)\right\|_2^2$$

A_T (l) and (A_S (l)) represent the educator and understudy models' separate actuations at the moderate layer l. The understudy model was additionally changed utilizing the LSDS misfortune during the subsequent step. While different choices for the refining position, directing layer, change works, and distance metric were as yet thought about during the execution and assessed as far as the viability of entire cancer division, despite the fact that this execution was viewed as the reference execution of our F D methodology.

V. RESULT AND DISCUSSION

In this section, the experimental outcomes of the proposed study is discussed to determine the efficacy of brain tumor segmentation using MRI through cross-model distillation process considerably.

5.1. Input Image

- FLAIR: T2-weighted FLAIR image, axial, coronal, 2–6 mm slice thickness.
- T1: T1-weighted, native image, sagittal with 1–6 mm slice thickness.
- T1c: T1-weighted, contrast-enhanced picture with an average patient voxel size of 1 mm.
- T2: T2-weighted image, with 2–6 mm slice thickness.

e-ISSN: 2582-5208
International Research Journal of Modernization in Engineering Technology and Science
(Peer-Reviewed, Open Access, Fully Refereed International Journal)
Volume:05/Issue:10/October-2023 Impact Factor- 7.868 www.irjmets.com

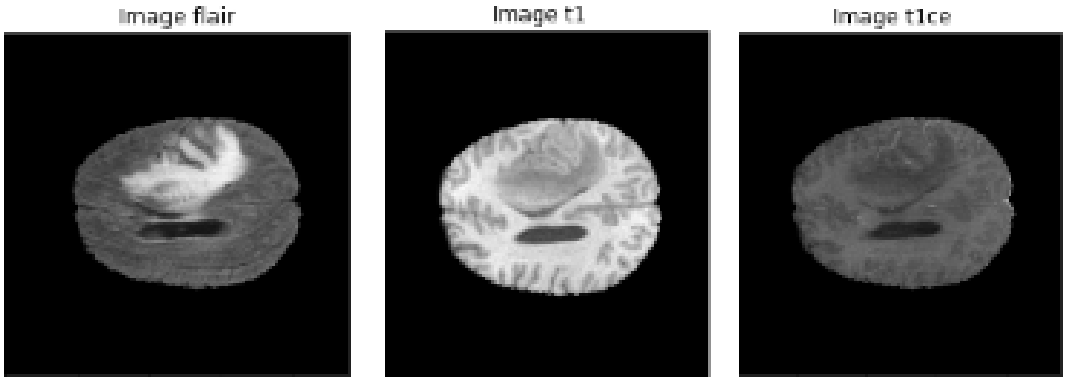

Figure 3. Input Image

5.2. Ground truth Image

Ground truth is expected to create ground truth information. The most common way of marking includes giving crude information names that depict what the information means. A managed learning model should be prepared utilizing the named yield. A more precise model is created by more exact naming. Manual naming of ground truth information can be tedious in light of the fact that numerous computer based intelligence models require thousands or millions of marked information results to produce precise outcomes.

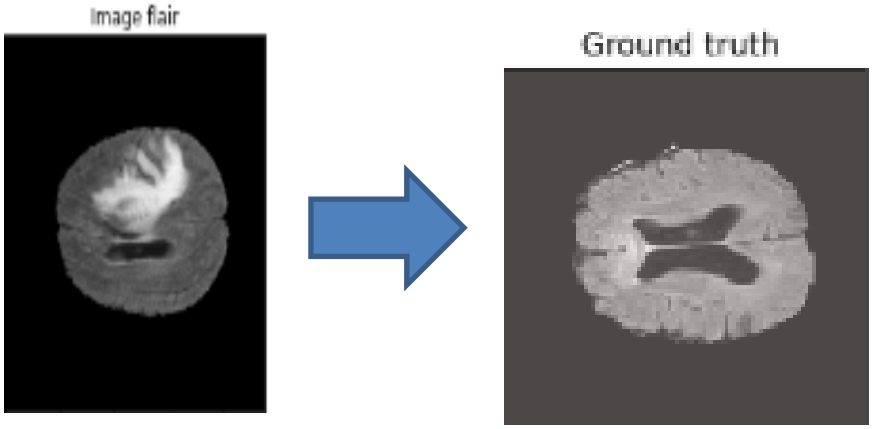

Figure 4. Ground truth Image

5.3. Classes

The below figure shows all classes of the brain image. Three type of SEGMENT_CLASSES are displayed in the image**.**

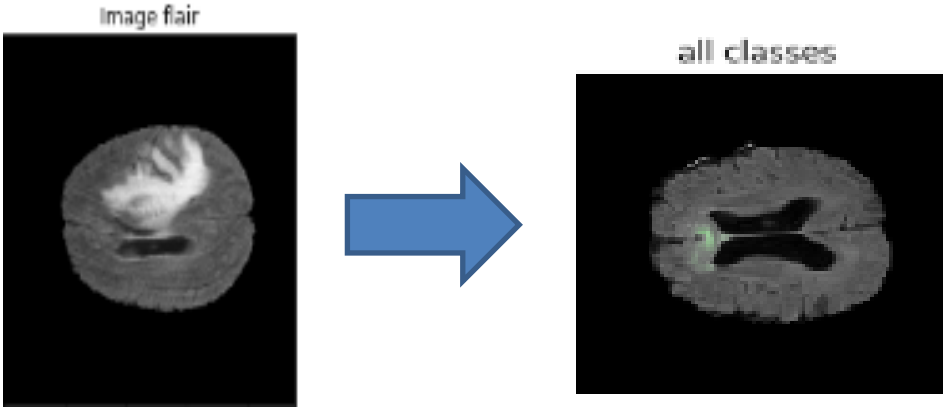

Figure 5. Classes

5.4. Prediction Type1

- The below figure shows the first prediction class of the brain image.

e-ISSN: 2582-5208
International Research Journal of Modernization in Engineering Technology and Science
(Peer-Reviewed, Open Access, Fully Refereed International Journal)
Volume:05/Issue:10/October-2023 Impact Factor- 7.868 www.irjmets.com

- It is a necrotic core tumour type.

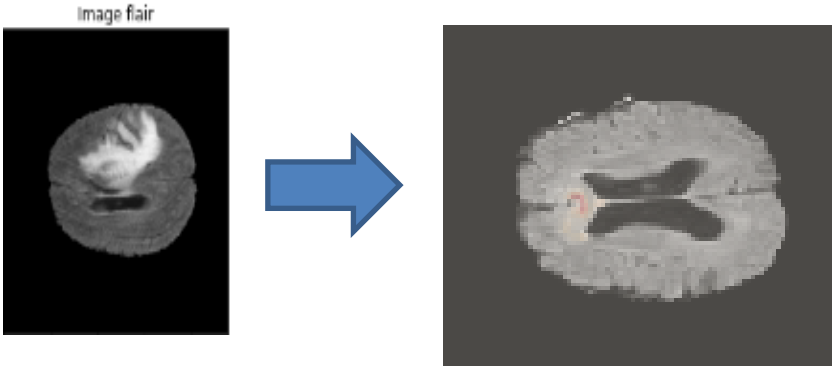

Figure 6. Prediction Type 1

5.5. Prediction Type 2

- The below figure shows the second prediction class of the brain image.
- It is an EDEMA type.

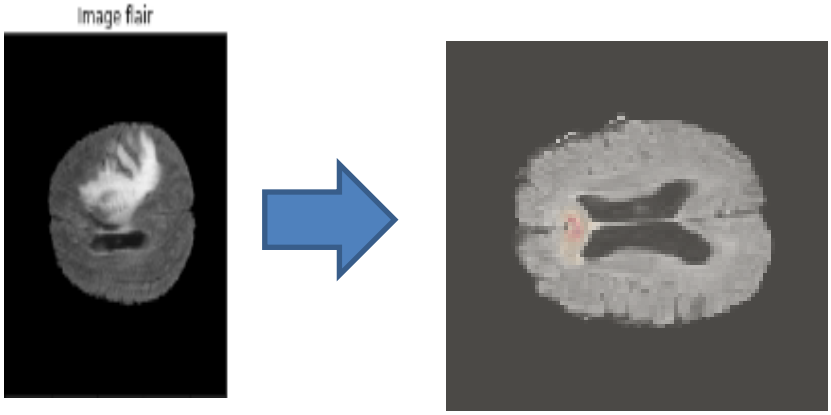

Figure 7. Prediction Type 2

5.6. Enhancing Predicted Image

- ✓ The below figure shows the enhancing predicted class of the brain image.
- ✓ In this class the result are more suitable for display or further image analysis.

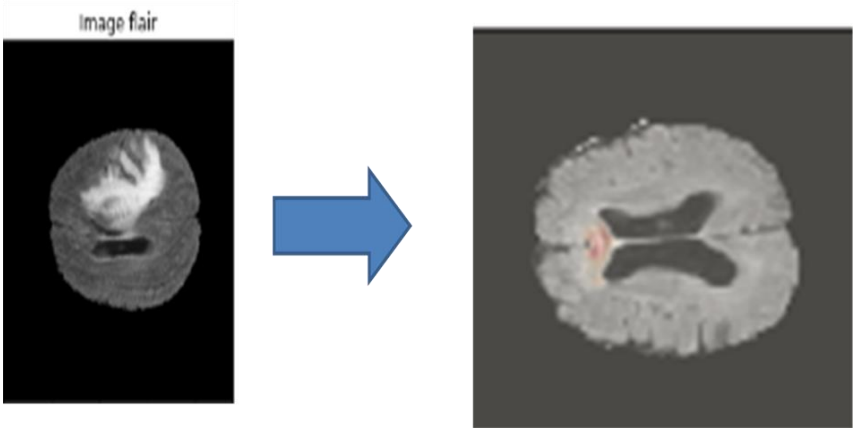

Figure 8. Enhancing Predicted Image

VI. PERFORMANCE ANALYSIS

6.1.Accuracy

- Various terms are every now and again utilized related to the meanings of responsiveness, explicitness, and exactness. Genuine Positive (TP), Genuine Negative (TN), Misleading Negative (FN), and Bogus Positive (FP) are

e-ISSN: 2582-5208
International Research Journal of Modernization in Engineering Technology and Science
(Peer-Reviewed, Open Access, Fully Refereed International Journal)
Volume:05/Issue:10/October-2023 Impact Factor- 7.868 www.irjmets.com

the four sorts. The experimental outcome is viewed as a veritable positive in the event that a sickness is demonstrated to be available in a patient and the given test likewise shows the presence of illness. Like how a patient's shortfall of an infection has been laid out, the test shows that the illness is likewise missing; this is known as a genuine negative (TN) result. Genuine positive and genuine negative proclamations infer a predictable result between the test and the laid out speculation (otherwise called the norm of truth). No clinical assessment, however, is immaculate. An experimental outcome is viewed as misleading positive (FP) on the off chance that it recognizes a sickness a not in a patient really have it.

- Like this, an experimental outcome is viewed as bogus negative (FN) on the off chance that it shows that a patient with a realized condition doesn't have it. The experimental outcomes are in conflict with the real illness when they are both dishonestly certain and erroneously negative. Responsiveness, explicitness, and exactness are abridged as TP, TN, FN, and FP.Accuracy = (TN + TP)/(TN+TP+FN+FP) = (Number of correct assessments)/Number of all assessments).

Table 1. Performance analysis of Accuracy

Methods	**Accuracy** (%)
D2-NET	98.35
CNN (U-NET)	99.93

The above table 1 shows the Performance analysis of Accuracy value of the existing and proposed system. The value of proposed system is higher.

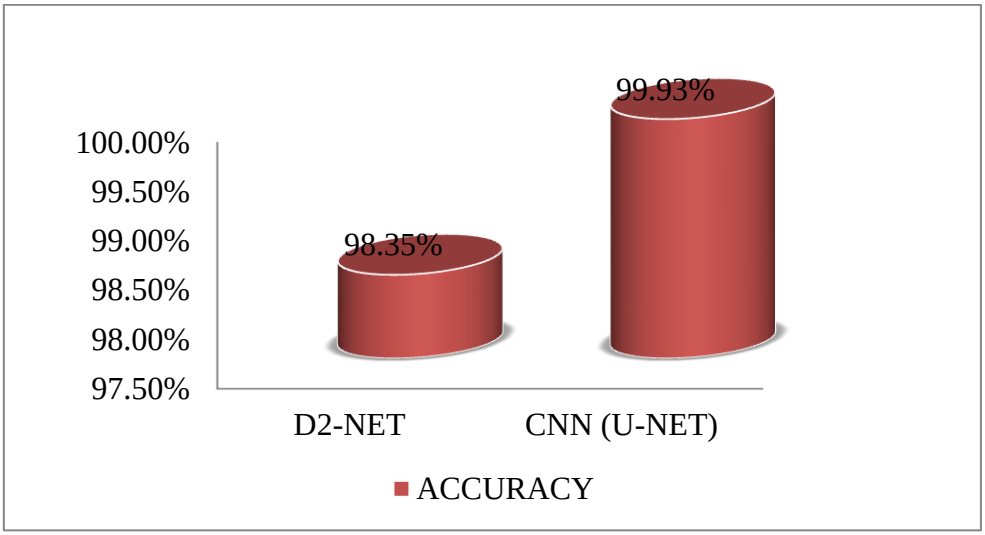

Figure 9. Performance analysis of Accuracy

VII. CONCLUSION

The Double Unraveling Organization, a remarkable strategy for mind cancer division in X-ray information, is presented by our concentrate as an end. Our model beats different methodologies by exploiting the unraveled portrayals, causing it a promising instrument for assisting clinical experts with recognizing and track problems related to mind growths. This examination can possibly have an impact past cerebrum growth division since unraveling techniques can be utilized for different picture handling position in the clinical business, extending the field of PC helped diagnostics and customized medication. To essentially work on persistent consideration and results, future review will focus on additional fostering the model and analyzing its application in genuine clinical settings.

VIII. REFERENCE

[1] M. Havaei et al., “Brain tumor segmentation with deep neural networks,” Med. Image Anal., vol. 35, pp. 18–31, Jan. 2017.

[2] H. Jia, Y. Xia, W. Cai, and H. Huang, “Learning high-resolution and efficient non-local features for brain glioma segmentation in MR images,” in Proc. MICCAI, 2020, pp. 480–490.

[3] C. Dai et al., "Suggestive annotation of brain tumour images with gradient-guided sampling," in Proc. MICCAI, 2020, pp. 156–165.
[4] B. Yu et al., "Learning sample-adaptive intensity lookup table for brain tumor segmentation," in Proc. MICCAI, 2020, pp. 216–226.
[5] J. Zhang, Y. Xie, Y. Wang, and Y. Xia, "Inter-slice context residual learning for 3D medical image segmentation," IEEE Trans. Med. Imag., vol. 40, no. 2, pp. 661–672, Feb. 2021.
[6] X. Guo, C. Yang, P. L. Lam, P. Y. Woo, and Y. Yuan, "Domain knowledge based brain tumor segmentation and overall survival prediction," in Proc. MICCAI Workshops, 2019, pp. 285–295.
[7] Q. Yang and Y. Yuan, "Learning dynamic convolutions for multi-modal 3D MRI brain tumor segmentation," in Proc. MICCAI Workshops, 2020, pp. 441–451.
[8] Y. Shen and M. Gao, "Brain tumor segmentation on MRI with missing modalities," in Proc. IPMI, 2019, pp. 417–428.
[9] K. van Garderen, M. Smits, and S. Klein, "Multi-modal segmentation with missing MR sequences using pre-trained fusion networks," in Proc. MICCAI Workshops, 2019, pp. 165–172.
[10] Y. Wang et al., "3D auto-context-based locality adaptive multi-modality GANs for PET synthesis," IEEE Trans. Med. Imag., vol. 38, no. 6, pp. 1328–1339, Jun. 2018.
[11] T. Zhou, H. Fu, G. Chen, J. Shen, and L. Shao, "Hi-Net: Hybrid-fusion network for multi-modal MR image synthesis," IEEE Trans. Med. Imag., vol. 39, no. 9, pp. 2772–2781, Sep. 2020.
[12] Y. Li, K. K. Singh, U. Ojha, and Y. J. Lee, "MixNMatch: Multifactor disentanglement and encoding for conditional image generation," in Proc. IEEE/CVF Conf. Comput. Vis. Pattern Recognit. (CVPR), Jun. 2020, pp. 8039–8048.
[13] C. Chen, Q. Dou, Y. Jin, H. Chen, J. Qin, and P.-A. Heng, "Robust multimodal brain tumor segmentation via feature disentanglement and gated fusion," in Proc. MICCAI, 2019, pp. 447–456.
[14] M. Havaei, N. Guizard, N. Chapados, and Y. Bengio, "HeMIS: Heteromodal image segmentation," in Proc. MICCAI, 2016, pp. 469–477.
[15] T. Zhou, S. Canu, P. Vera, and S. Ruan, "Latent correlation representation learning for brain tumor segmentation with missing MRI modalities," IEEE Trans. Image Process., vol. 30, pp. 4263–4274, 2021.
[16] J. Ouyang, E. Adeli, K. M. Pohl, Q. Zhao, and G. Zaharchuk, "Representation disentanglement for multi-modal brain MRI analysis," in Proc. IPMI, 2021, pp. 321–333.
[17] Q. Wang, L. Zhan, P. Thompson, and J. Zhou, "Multimodal learning with incomplete modalities by knowledge distillation," in Proc. 26th Int. Conf. Knowl. Discovery Data Mining, Aug. 2020, pp. 1828–1838.
[18] T. Xia, A. Chartsias, and S. A. Tsaftaris, "Pseudo-healthy synthesis with pathology disentanglement and adversarial learning," Med. Image Anal., vol. 64, Aug. 2020, Art. no. 101719.
[19] Q. Suo, W. Zhong, F. Ma, Y. Yuan, J. Gao, and A. Zhang, "Metric learning on healthcare data with incomplete modalities," in Proc. 28th Int. Joint Conf. Artif. Intell., Aug. 2019, pp. 3534–3540.
[20] B. Zhan, D. Li, X. Wu, J. Zhou, and Y. Wang, "Multi-modal MRI image synthesis via GAN with multi-scale gate mergence," IEEE J. Biomed. Health Informat., vol. 26, no. 1, pp. 17–26, Jan. 2022.
[21] Roy, S., He, Q., Sweeney, E., Carass, A., Reich, D.S., Prince, J.L. and Pham, D.L., 2015. Subject-specific sparse dictionary learning for atlas-based brain MRI segmentation. IEEE journal of biomedical and health informatics, 19(5), pp.1598-1609.
[22] Dubey, Y.K., Mushrif, M.M. and Mitra, K., 2016. Segmentation of brain MR images using rough set based intuitionistic fuzzy clustering. Biocybernetics and biomedical engineering, 36(2), pp.413-426.
[23] Zhang, J., Liu, M., An, L., Gao, Y. and Shen, D., 2017. Alzheimer's disease diagnosis using landmark-based features from longitudinal structural MR images. IEEE journal of biomedical and health informatics, 21(6), pp.1607-1616.
[24] Dong, B., Jin, R. and Weng, G., 2019. Active contour model based on local bias field estimation for image segmentation. Signal Processing: Image Communication, 78, pp.187-199.
[25] Pereira, S., Pinto, A., Amorim, J., Ribeiro, A., Alves, V. and Silva, C.A., 2019. Adaptive feature recombination and recalibration for semantic segmentation with fully convolutional networks. IEEE transactions on medical imaging, 38(12), pp.2914-2925.

[26] Wang, Guotai, Wenqi Li, Sébastien Ourselin, and Tom Vercauteren. "Automatic brain tumor segmentation using cascaded anisotropic convolutional neural networks." In Brainlesion: Glioma, Multiple Sclerosis, Stroke and Traumatic Brain Injuries: Third International Workshop, BrainLes 2017, Held in Conjunction with MICCAI 2017, Quebec City, QC, Canada, September 14, 2017, Revised Selected Papers 3, pp. 178-190. Springer International Publishing, 2018.

[27] Isensee, F., Kickingereder, P., Bonekamp, D., Bendszus, M., Wick, W., Schlemmer, H.P. and Maier-Hein, K., 2017. Brain tumor segmentation using large receptive field deep convolutional neural networks. In Bildverarbeitung für die Medizin 2017: Algorithmen-Systeme-Anwendungen. Proceedings des Workshops vom 12. bis 14. März 2017 in Heidelberg (pp. 86-91). Springer Berlin Heidelberg.